

Formation of Highly Structured Cubic Micellar Lipid Nanoparticles of Soy Phosphatidylcholine and Glycerol Doleate and Their Degradation by Triacylglycerol Lipase

Maria Wadsäter,^{*,†} Justas Barauskas,^{‡,§} Tommy Nylander,[†] and Fredrik Tiberg^{†,‡}

[†]Department of Physical Chemistry, Lund University, P.O. Box 124, SE-22100 Lund, Sweden

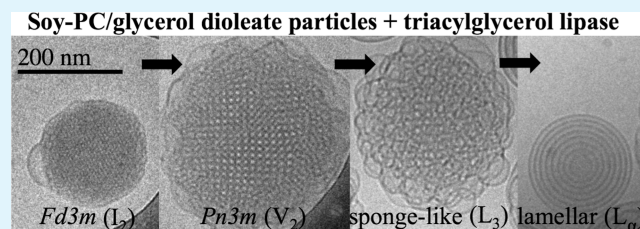
[‡]Camurus AB, Ideon Science Park, Gamma Building, Sövegatan 41, SE-22379 Lund, Sweden

[§]Biomedical Science, Faculty of Health and Society, Malmö University, SE-20506 Malmö, Sweden

Supporting Information

ABSTRACT: Lipid nanoparticles of reversed internal phase structures, such as cubic micellar (I_2) structure show good drug loading ability of peptides and proteins as well as some small molecules. Due to their controllable small size and inner morphology, such nanoparticles are suitable for drug delivery using several different administration routes, including intravenous, intramuscular, and subcutaneous injection. A very interesting system in this regard, is the two component soy phosphatidylcholine (SPC)/glycerol dioleate (GDO) system, which depending on the ratio of the lipid components form a range of reversed liquid crystalline phases. For a 50/50 (w/w) ratio in excess water, these lipids have been shown to form a reversed cubic micellar (I_2) phase of the $Fd3m$ structure. Here, we demonstrate that this SPC/GDO phase, in the presence of small quantities (5–10 wt %) of Polysorbate 80 (P80), can be dispersed into nanoparticles, still with well-defined $Fd3m$ structure. The resulting nanoparticle dispersion has a narrow size distribution and exhibit good long-term stability. In pharmaceutical applications, biodegradation pathways of the drug delivery vehicles and their components are important considerations. In the second part of the study we show how the structure of the particles evolves during exposure to a triacylglycerol lipase (TGL) under physiological-like temperature and pH. TGL catalyzes the lipolytic degradation of acylglycerides, such as GDO, to monoglycerides, glycerol, and free fatty acids. During the degradation, the interior phase of the particles is shown to undergo continuous phase transitions from the reversed I_2 structure to structures of less negative curvature (2D hexagonal, bicontinuous cubic, and sponge), ultimately resulting in the formation of multilamellar vesicles.

KEYWORDS: *cubic micellar nanoparticles, lipids, liquid crystals, intravenous, parenteral, drug delivery, triacylglycerol lipase and phase transitions*



INTRODUCTION

Reversed nonlamellar liquid crystalline (LC) phases of lipids, such as the cubic micellar (I_2), 2D-hexagonal (H_2), bicontinuous cubic (V_2), and “sponge” (L_s) phase, form spontaneously from many polar lipid–water systems.^{1,2} Due to the nanostructure, comprising space-divided lipid and aqueous domains, reversed lipid LC structures have for a long time been recognized as promising biocompatible materials in various different drug delivery applications since they can solubilize and efficiently encapsulate many different types of molecules (hydrophilic, hydrophobic, and amphiphilic molecules) but also protect the active substances from rapid biodegradation upon administration.³

Nonlamellar lipid LC nanoparticles (LCNPs), prepared by dispersing LC phases in the presence of stabilizer, are due to their small size promising for several different administration routes, including parenteral delivery, where they may be exploited as carriers and for solubilization and/or encapsulation of various drug compounds, resulting in sustained release,

extended circulation and/or passive targeting of disease sites.^{4–7} Here, the ability of a LC phase or its nanoparticles to encapsulate a substance is known to be highly dependent on its degree of domain connectivity, since this determines the freedom of enclosed molecules to diffuse within and out from the liquid crystals. A phase with small discrete water domains, such as the I_2 phase,⁸ is thus expected to exhibit the most extended drug release profiles and thereby prolonged therapeutic concentrations in the body.⁶ Although various LCNPs of V_2 ,⁹ H_2 ,¹⁰ and L_3 ¹¹ structure can be prepared relatively easily using mixtures of monoglycerides with other acylglycerides, their use in intravenous administration is not optimal due to the concentration dependent hemolytic activity and associated toxicity of monoglycerides.¹²

Received: December 18, 2013

Accepted: April 29, 2014

Published: April 29, 2014

In this regard, an alternative nanoparticle forming system comprising soy phosphatidylcholine (SPC) and glycerol dioleate (GDO) has been developed. Due to the two-component nature of this system, it can be used to tune in different functional phase structures depending on the ratio of the two lipids (the H_2 and I_2 phase is formed in excess of water at particular SPC/GDO ratios).^{13–16} Recently LCNPs based on SPC/GDO were prepared using an amphiphilic polymeric surfactant polyoxyethylene (20) sorbitan monooleate (Polysorbate 80 or P80) at concentrations of 15–20 wt % with respect to total lipid and P80 amount.¹⁷ When compared to monoglycerides the SPC/GDO LCNPs have negligible hemolytic activity and are nontoxic at relatively high doses, making them suitable also for parenteral administration routes.^{12,17} In the efforts to develop the SPC/GDO-based LCNPs for parenteral drug delivery applications, extensive studies on their interaction with model lipid membranes⁵ and with blood^{12,18} were conducted to understand their characteristic interactions with biological interfaces and components. This system was also demonstrated to be applicable, for example, the *in vivo* parenteral delivery of somatostatin, propofol, and docetaxel.^{4,5,17} Pharmacokinetic of both somatostatin and propofol in rats showed sustained high blood levels when injected in SPC/GDO LCNPs compared to in buffer solution or other commercial internally structured particle systems.^{5,17}

Nevertheless, the internal I_2 LC structure of the used particles was never demonstrated by any direct measurements, and the particles were proposed to be of the I_2 phase based only on the SPC/GDO/water phase diagram.¹⁵ In the first part of the present study, we show by synchrotron small-angle X-ray diffraction (SAXD) that the dispersion agent P80 interacts with lipids and has a disordering effect on the internal LCNP structure and that the P80 concentrations must be kept relatively low (in the order of 5–10 wt % relative total amount of lipid and P80) to obtain well-defined and highly structured I_2 LCNPs prepared at a SPC/GDO weight ratio of 50/50.

In the second part of this study, we focused on understanding the biodegradation process of the SPC/GDO LCNPs upon intravenous administration, where after the LCNPs eventually will be exposed to lipolytic degradation,¹⁹ giving direct consequences on the internal LC structure and thus the encapsulation abilities of the particles, yet to be explored.

Ever since the early observations by Patton et al.²⁰ that dietary fat (triglycerides) form several different lipid LC phases during the digestion by pancreatic lipase, plenty of studies on LC phase and colloidal transformations during the digestion of more simple emulsions of acylglycerides under physiological conditions present in the intestine have been conducted. For instance, bile salt concentration, pH (i.e., the degree of protonation of the fatty acids), and buffer conditions were found to play an important role both for the kinetics of the lipolysis and the LC nanostructure.^{21–23}

Since both GDO and PCs are naturally occurring lipids with well-known metabolic pathways, the biodegradation of the SPC/GDO LCNPs after intravenous injection is expected to be a complex process, influenced both by triacylglycerol lipases (TGL) and phospholipases. In order to model, predict, and gain a mechanistic insight into the biodegradation of SPC/GDO-based LCNPs and the associated structural transformations and kinetics, we have chosen to study the effects of the two main classes of lipases, separately. In this first paper, the focus is on the effect of the GDO hydrolysis on the

structure and stability of highly structured I_2 SPC/GDO LCNPs. Herein, porcine pancreas TGL constitutes a model lipase, which activity results in GDO hydrolysis with expected effects on the internal structure of the LCNPs. These were studied by time-resolved synchrotron SAXD, cryo-TEM, and dynamic light scattering (DLS).

EXPERIMENTAL METHODS

Materials. SPC, GDO, and P80 were purchased from Lipoid, Danisco, and Croda, respectively. The purity of the SPC (denoted as SPC S100) was 97.6% and the hydrocarbon chain composition was 12–17% palmitic acid, 2–5% stearic acid, 7–12% oleic acid, 59–70% linoleic acid, and 5–8% linolenic acid, according to the producer. The GDO (denoted as Rylo DG 20 Pharma) contained minimally 85% diglycerides and maximally 10 and 5 and 1% mono- and triglycerides and free glycerol, respectively, according to the producer. Furthermore, minimally 89% of the fatty acids were oleic acid. Ethanol and propylene glycol were purchased from Sövete and Fisher, respectively. All chemicals were used without further purification. Sterile water was obtained from Apoteket (Sweden) and porcine pancreas lipase (type VI) was purchased from Sigma-Aldrich.

Sample Preparation. All sample compositions herein are given as percentages by weight, unless otherwise stated. SPC and GDO were mixed with ethanol (EtOH) and propylene glycol (PG) (42.5/42.5/10/5 SPC/GDO/EtOH/PG) to reduce the viscosity of the lipid mixture. The dispersant, P80 was added to the lipid solution (P80/lipid solution 5/95). The lipid solution was added to sterile water (5/95 (lipid+P80)/H₂O) followed by immediate vigorous shaking for >5 days at room temperature. The lipid LC phase were thereby coarsely fragmented into homogeneous dispersions, which were further fragmented when passed five times through a Microfluidizer 110S (Microfluidics Corp., Newton, MA) at 5000 PSI. The dispersions were then autoclaved (CertoClav CV-EL, CertoClav Sterilizer GmbH, Traun, Austria) at 125 °C and a pressure of 1.4 bar for approximately 30 min and finally filtered using 5 μm Versapor membrane syringe filters (PALL Life Science) to remove any large aggregates, sometimes formed at the air–water interface.

Structural Studies of the Degradation of LCNPs Catalyzed by TGL. Lipid dispersion, TGL, and 0.2 M tris buffer was mixed to yield a reaction mixture containing 17.7 mg/mL lipid and 0.17 mg/mL TGL in 0.12 M tris at pH 7.5. The reaction mixture was immediately loaded into the dynamic light scattering or SAXD cells preheated to 37 °C. In case of cryo-TEM, the reaction mixtures were incubated at 37 °C until depositing the sample on the electron microscope grid. The pH (7.5) was the same after the reaction, which confirms that the used tris concentration was sufficiently high to buffer the produced fatty acid.

Synchrotron Small-Angle X-ray Diffraction. SAXD measurements were performed at beamline I911-4 at MAX-lab, Sweden. Dispersions were injected to capillary cells and bulk LC references loaded to steel sample holders and sealed with kapton windows. The sample was mounted 1952 mm from the 1 M PILATUS 2D detector. The X-ray wavelength was 0.91 Å, and the size of the beam at the sample was approximately 0.25 × 0.25 mm. Diffractograms of the dispersions and bulk phases were recorded during 3 min, while 1 min measurements were used in the study of the LCNP degradation by TGL. The intensities recorded by the 2D detector were integrated using Fit2D provided by A. Hammersley (<http://www.esrf.eu/computing/scientific/FIT2D/>).

Dynamic Light Scattering. The size distribution of dispersions diluted in H₂O to 0.5 wt % at 25 and 37 °C were measured using a DLS (Zetasizer Nano ZS, Malvern Instruments). The effect of the TGL catalyzed reaction was monitored at 37 °C every 5 min for approximately 5 h. Autocorrelation functions were analyzed using instrument software (Malvern Instruments Ltd.) using the default General Purpose model. The mean particle size (intensity averaged) was then reported.

Cryogenic Transmission Electron Microscopy. The morphology of the LCNP before and after incubation with TGL at 37 °C was

studied with cryo-TEM. The temperature ($25\text{--}28\text{ }^{\circ}\text{C}$) and relative humidity (close to saturation) of the sample vitrification system was controlled to favor the formation of a proper vitreous film and avoid evaporation in the sample during preparation. Five microliters of 1.5–2 wt % LCNP solutions were placed on the carbon film supported by a copper grid and blotted with filter paper to reduce film thickness. The grid was quenched in liquid ethane at $-196\text{ }^{\circ}\text{C}$, stored under liquid nitrogen ($-196\text{ }^{\circ}\text{C}$), and transferred to a cryo-TEM (Philips CM120 BioTWIN Cryo) equipped with a postcolumn energy filter (Gatan GIF 100), using an Oxford CT3500 cryoholder and its workstation. The acceleration voltage was 120 kV and the working temperature was below $-180\text{ }^{\circ}\text{C}$. The images were digitally recorded with a CCD camera (Gatan MSC 791) under low-dose conditions. The underfocus was approximately 1 μm .

■ RESULT AND DISCUSSION

Structure of 50/50 SPC/GDO LCNPs. Mixtures of SPC and GDO show rich phase behavior, where the occurrences of different polymorphic forms can be tuned by changing the SPC/GDO ratio. For decreasing SPC/GDO ratio lamellar (L_a), H_2 , I_2 , and disordered micellar (L_2) phases are observed, which all exist in equilibrium with excess water.^{15,16} Dispersions of 50/50 SPC/GDO were prepared using 5, 7.5, 10, and 15% P80 and their LC structure was probed by SAXD, see Figure 1.

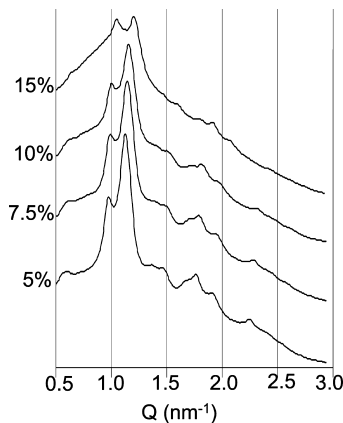


Figure 1. SAXD of 50/50 SPC/GDO dispersions with 5, 7.5, 10, and 15% P80 at $25\text{ }^{\circ}\text{C}$.

Here, it should be noted that the internal LC structure of the used particles were never demonstrated by any direct measurements. The LCNPs dispersed with 5% P80 give rise to 9 distinct Bragg reflections with relative positions, $\sqrt{3}:\sqrt{8}:\sqrt{11}:\sqrt{16}:\sqrt{19}:\sqrt{24}:\sqrt{27}:\sqrt{32}:\sqrt{44}$, which can be indexed as the diffraction from a face-centered cubic micellar phase of the $Fd\bar{3}m$ space group.^{8,24,25} In this study, we are for the first time reporting on well-defined highly structured cubic micellar ($Fd\bar{3}m$) SPC/GDO/P80 nanoparticles as shown by SAXD, corresponding to LC structure of the bulk 50/50 SPC/GDO equilibrium phase.¹⁶ For increasing fraction of P80 (7.5 and 10%), the Bragg reflections of the I_2 nanoparticles gradually become less distinct and intense and are almost lost at 15% P80, indicating increased structural disorder (formation of L_2 phase). Moreover, the repeat distance (lattice parameter) of the crystalline structure of the nanoparticles decreases for increasing fraction of P80 and is 18.1, 17.9, 17.8, and 16.9 nm for 5, 7.5, 10, and 15% P80, respectively. The corresponding value for the bulk 50/50 SPC/GDO equilibrium phase is 18.7 nm.¹⁶

The polymeric surfactant P80 can disperse bulk liquid crystals and stabilize dispersed LCNPs by reducing the surface free energy of the particles. P80 is thus expected to mainly reside at the surface of the particles and likely also as micelles in the solution (CMC 0.014 mM).²⁶ However, the trends of decreasing lattice parameter and peak broadening with increasing P80 concentration (Figure 1) suggest that an increasing fraction penetrate the lipid matrix and solubilizes lipids from the particle interior at higher P80 concentrations. Interestingly, one would based on the SPC/GDO/water phase diagram,¹⁵ expect that a decreasing fraction of SPC would result in a lower degree of hydration and hence decreasing lattice parameter, while a L_2 phase would be formed upon depletion of SPC (at 80% GDO).¹⁶ SAXD studies of the bulk LC phase of 50/50 SPC/GDO with increasing fraction of P80 showed a disordered micellar phase at 20% P80 followed by a lamellar phase at 30% P80.²⁷ For nanoparticles, cryo-TEM studies showed that the use of an increased fraction of P80 (10–30%) to disperse diglycerol monooleate/GDO bulk crystals resulted in nanoparticles with an increasingly thick corona of disordered extended multiply connected bilayers at the expense of the volume of the denser particle core.¹¹ Similar swollen coronas were apparent also in cryo-TEM images for SPC/GDO particles containing 15–20% P80.^{17,28} High fractions of P80 is thus suggested to induce phase separation yielding a P80 and SPC rich phase, which goes to the particle surface and form the corona of interconnected lamellar structures. Consequently, the particle interior will contain a higher fraction of GDO, giving decreased hydration, lattice parameter and LC order with increasing P80 fraction.

Thus, the fraction of P80 in the lipid mixture must be carefully balanced to be low enough not to affect the LC structure of the particles but still be high enough to efficiently disperse the bulk crystal. Indeed, DLS measurements of the SPC/GDO LCNPs dispersed with 5, 10, and 15% P80, all yielded monomodal and narrow (polydispersity index of 0.004, 0.032, and 0.006, respectively) size distributions with relatively similar average particle sizes, 206, 186, and 195 nm, respectively (Figure 2). Thus, 5% P80 is sufficient to efficiently disperse the 50/50 SPC/GDO bulk crystal and yields highly structured I_2 nanoparticles. Moreover, both the $Fd\bar{3}m$ structure (Supporting Information (SI) Figure SI 1A) and the average particle size and polydispersity index (Figure SI 1B) for these LCNPs were preserved for at least for 6 months after preparation. This verify that the LCNPs containing 5% P80 showed a high stability

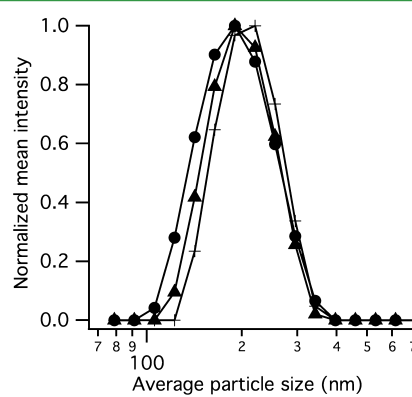


Figure 2. Size distribution of the 50/50 SPC/GDO dispersions containing 5 (crosses), 10 (circles), and 15 (triangles) % P80 at $25\text{ }^{\circ}\text{C}$, as measured by DLS.

both in terms of LC phase and particle integrity. Here, it should be emphasized that the preparation of such highly structured and stable LCNPs with narrow monomodal size distributions is nontrivial, as reflected by the very few reports in the past, including also other lipidic systems. The LCNPs of mixtures of SPC and vitamin E is to the best of our knowledge the only previous system for which such structured cubic micellar ($Fd3m$) has been obtained.²⁹

Studies of the morphology of the LCNPs with 5% P80 by cryo-TEM (Figure 3A and B) revealed well-defined dense

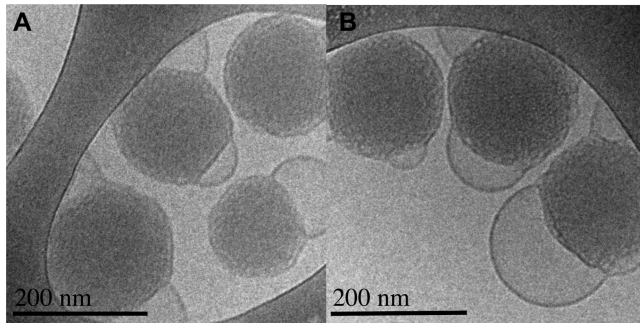


Figure 3. (A and B) Representative cryo-TEM images of 50/50 SPC/GDO nanoparticles, dispersed using 5% P80.

spherical particles. The I_2 structure is, due to its nature, challenging to image as it is composed of very small closely packed reversed micelles, resulting in a relatively low fraction of water.¹⁷ Moreover, in contrast to the water domains of, for example, the H_2 and V_2 phases, the micelles of the I_2 phase constitute closed water compartments, which reduces contrasts between lipid and water domains and therefore imaging is more challenging than for LCNPs of the H_2 or V_2 phase.^{30,31} Additionally, as the particles are spherical they are not aligning in any particular orientation on the grid surface and the probability of viewing the LCNPs in correct angle, in respect to crystal structure, is expected to be low.

A few vesicle-like structures are attached to the well-defined surface of the LCNPs. Petal-like shells of vesicles, which were suggested to be enriched with P80, were previously observed with cryo-TEM for 50/50 SPC/GDO particles dispersed with 20% P80. The few vesicles present on the particle can thus be an effect of P80 excess at the surface or a consequence of the blotting procedure during sample preparation.

Degradation of the I_2 SPC/GDO Nanoparticles by Porcine TGL. Stable and highly structured I_2 LCNPs are attractive systems for many different drug delivery applications and routes of administration. However, regardless of administration route the LCNPs will eventually encounter the lipases of the human body, which will affect the LC compositions and structure of the particles and thus their functionality (e.g., drug encapsulation). In the present study, we focus on the effect of TGL catalyzed degradation of GDO on the I_2 structure, integrity, and morphology of the 50/50 SPC/GDO nanoparticles dispersed with 5% P80. Full hydrolysis of GDO yields free OA and glycerol, via the intermediate, GMO.^{32–34} Consequently, phase transitions may be expected for the I_2 nanoparticles upon *in vivo* administration. As the focus of this study is on the parental route of delivery, bile salts were not included in our lipolysis assay. Furthermore, the lipolytic activity of TGL on phospholipids is expected to be negligible.

The progress of the structural degradation of the SPC/GDO particles at pH 7.5 and 37 °C is shown in Figure 4, as a

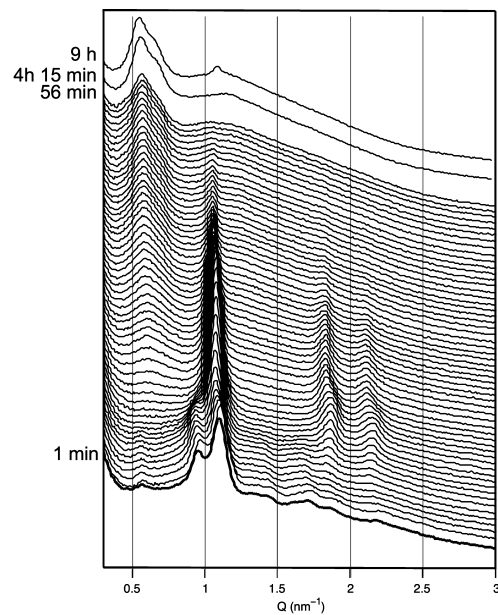


Figure 4. SAXD data showing the effect of TGL-catalyzed degradation of 50/50 SPC/GDO LCNPs in 0.12 M Tris at pH 7.5 and 37 °C. The lipase free reference is shown as a thick line. Diffractograms were initially recorded every minute for 56 min after addition of TGL. Additional diffractograms were then recorded after 4 h 15 min and 9 h.

continuous phase transition between several LC phases, as measured by SAXD. The diffraction pattern from the intact $Fd3m$ LCNPs turn, within a few minutes, into three distinct Bragg reflections with relative positions, $\sqrt{1}:\sqrt{3}:\sqrt{4}$, corresponding to a 2D hexagonal phase.

A broad intensity peak at $q \sim 0.6 \text{ nm}^{-1}$ starts to emerge after about 15 min and grows stronger in intensity as the H_2 reflections diminish. Since the progress of the reaction may vary between different particles and also within individual particles, for example, between particle surface and interior, the continuous degradation of the LCNPs is expected to result in a coexistence of several different LC phases. As a consequence, the scattering will be diffuse and just give rise to broad peaks or shoulders in the diffractogram. However, upon further progress of the reaction (after 4 h 15 min), a shoulder is discernible on the right side of the broad peak (now positioned at $q \sim 0.55 \text{ nm}^{-1}$). The relative positions of the two superimposed peaks, $\sqrt{2}:\sqrt{3}$, can be indexed as the first two reflections from a V_2 structure of the $Pn3m$ space group. Cryo-TEM images obtained after 1.5 h of TGL catalysis (Figure 5A and B) show larger partly ordered particles, enclosed by a corona of uncompact interconnected lipid bilayers. The LC structure of the particles are more hydrated than the intact I_2 LCNPs and resembles previously depicted dispersions (1:1:4 egg PC:lyso-PC:OA), which were suggested to be of a bicontinuous cubic phase.³⁵ Several domains of bicontinuous cubic structures with different orientation are visible in single particles in Figure 5. Small differences in for instance lattice constant among these domains are also contributing to the broadening of the SAXD peaks in Figure 4.

After additional time of lipase action (8 h), cryo-TEM images (Figure 5C and D) show a mixture of sponge-like¹¹ particles with disordered interconnected bilayers, well-defined multi-

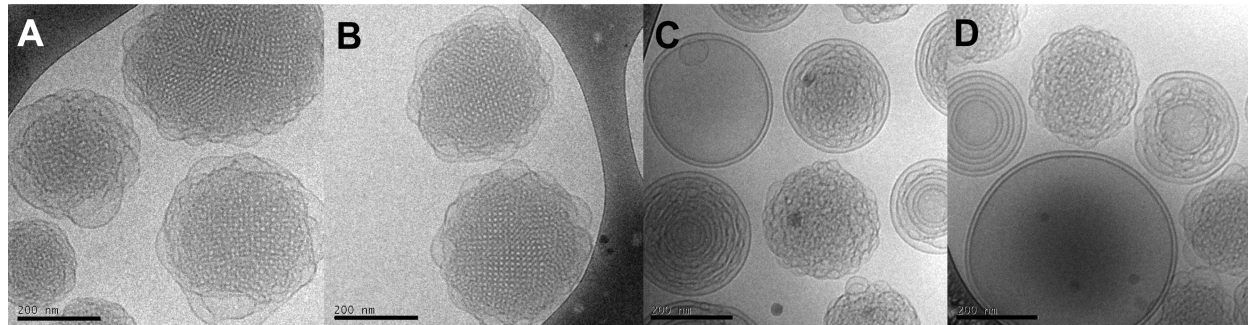


Figure 5. Cryo-TEM images of 50/50 SPC/GDO nanoparticles in 0.12 M tris and pH 7.5 degraded by TGL at 37 °C for (A and B) 1.5 and (C–D) 8 h. The scale bar is 200 nm in all images.

lamellar structures, and intermediates of these. Again the coexistence of several LC phases explains the relatively diffuse diffraction pattern observed after 9 h by SAXD (Figure 4). However, a new distinct peak has emerged at $q = 1.1 \text{ nm}^{-1}$. As the q -value of this peak is twice as large as for the $q = 0.55 \text{ nm}^{-1}$ peak, this supports the presence of a lamellar phase, for which the positions of the diffraction peaks are simply integers (1, 2, 3...) of the position of the first peak.

In the course of the phase transitions induced by the catalytic activity of TGL, the lattice constant of the I_2 crystal increases from 18.7 nm to maximally 19.5 nm before the transition to the H_2 phase occurs (Figure 6). For the H_2 phase the lattice

During the TGL catalyzed hydrolysis of GDO, the degradation of the 50/50 SPC/GDO results in a pathway through several LC structures ($I_2 \rightarrow H_2 \rightarrow V_2 \rightarrow L_3/L_a$) of gradually decreasing negative curvature. This is not surprising as PC is known to be a lamellar forming lipid¹⁵ and both GMO and OA form structures of less negative curvature than glycerol dioleate.^{36,37} In addition, investigations of TGL catalyzed degradation of LCNPs with different SPC/GDO ratios showed that the same pathway of phase transitions was followed, although the initial structure differed (see Figure SI 2). In equilibrium with water, GMO forms a bicontinuous cubic phase at 37 °C,³⁸ while the overall aggregate structure of OA is highly dependent on the protonation state of the fatty acid as well as the sample composition.³⁹ However, lamellar structures were reported to dominate in dilute (H_2O) systems of both pure OA and at equimolar composition of egg PC and OA at 25 °C and pH 7.4, at which OA is expected to be only partly protonated.³⁵ A 100% complete hydrolysis of the GDO in the 50/50 SPC/GDO LCNPs would result in an approximate molar composition of 3:7 PC/OA. The final destination for such completely hydrolyzed SPC/GDO particles by TGL is thus most likely a lamellar phase. However, although a lamellar phase was detected by SAXD (Figure 4) and cryo-TEM (Figure 3), conclusions regarding the completion of the GDO and GMO hydrolysis, cannot be drawn. This requires complex analysis of the composition or in depth studies of the phase behavior for mixtures of PC, GDO, GMO, and OA. As we expect, most of the encapsulated drug in SPC/GDO LCNPs already to be released when the lamellar phase is reached, such studies where not conducted.

This study presents insights to the structural degradation of the I_2 50/50 SPC/GDO particles in respect to the lipolysis of GDO by TGL. As a consequence of the GDO hydrolysis, several phase transitions occur in the SPC/GDO LC structure, but the integrity of the nanoparticles is typically retained during the reaction. This confirms that P80 is an efficient stabilizer, but it does not significantly hamper the TGL catalyzed lipolysis. Although TGL is the most important enzyme for the degradation of one of the major components in the LCNPs, the GDO, several other factors may affect the stability of the particles *in vivo*. For instance, phospholipases, which catalyzes the lipolysis of phospholipids such as SPC, are also expected to attack the nanoparticles and are currently being investigated in our group.

CONCLUSIONS

Highly structured I_2 nanoparticles have been shown to have good drug encapsulation ability of peptides and small

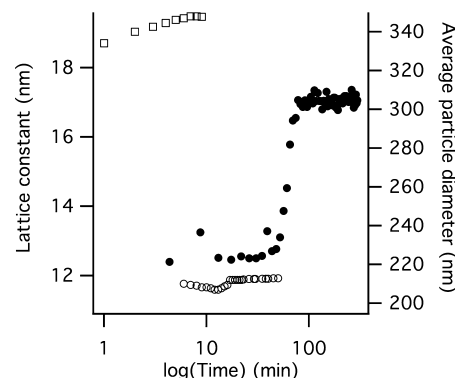


Figure 6. Average particle size (filled circles) during degradation of 50/50 SPC/GDO LCNPs in 0.12 M tris and pH 7.5 by TGL at 37 °C as measured by dynamic light scattering. The change in lattice constant of the I_2 (open squares) and H_2 phase (open circles) during the degradation by TGL is also shown.

constant further increases from 6.7 to 6.9 nm during the period of time when it is detectable by SAXD. DLS was used to monitor the size of the LCNPs during the TGL catalyzed phase transitions (Figure 6). No significant change in particle size was measured during the transition from the I_2 to H_2 phase (~ 10 min). After 60 min of TGL catalyzed lipolysis, the particle size rapidly (within 20 min) increased by 50% to approximately 300 nm. Similar particle sizes were deduced from cryo-TEM images obtained before (Figure 3) and after (1.5 and 8 h) incubation with TGL (Figure 5). The abrupt increase in particle size occurs at a stage, where the Bragg reflections of the H_2 phase are completely lost and the V_2 phase is forming. Thus, the increase in particle size is most likely coupled to the absorption of water in the LC structure during the formation of the V_2 phase, which is significantly more hydrated than both the I_2 and H_2 phases.

molecules, as compared to particles of LC phases with continuous aqueous and lipid nanodomains. They are therefore attractive candidates for several drug delivery applications.⁶ In the present study, cubic micellar (*Fd3m*) nanoparticles of 50/50 SPC/GDO with a narrow monomodal size distribution are prepared using a low fraction (5–10%) of the dispersing agent P80. At this low fraction, the same LC structure is observed for the particles as for the 50/50 SPC/GDO phase diagram. Higher fractions of P80 results in increased structural disorder. In the second part of this study, the effect of the lipolytic degradation of GDO by TGL on the I₂ nanoparticles under physiological pH and temperature was investigated with respect to LC structural transitions and morphology changes of the particles. In conclusion, as the GDO is degraded to GMO and, eventually further to OA and glycerol, the particles undergo continuous phase transitions from the I₂ structure to LC structures of gradually less negative curvature. The *Fd3m* structure is successively transformed in to the H₂, V₂, and L₃ phase, before a lamellar phase structure finally is observed. The particles are retained as discrete structures throughout the whole degradation process, while their averaged size increases with approximately 50%.

■ ASSOCIATED CONTENT

Supporting Information

SAXD and DLS data showing nanoparticle stability and SAXD data of TGL catalyzed degradation of 40/60 and 60/40 SPC/GDO nanoparticles. This material is available free of charge via the Internet at <http://pubs.acs.org>.

■ AUTHOR INFORMATION

Corresponding Author

*Email: maria.wadsater@fkem1.lu.se.

Notes

The authors declare no competing financial interest.

■ ACKNOWLEDGMENTS

This work was financed by the Swedish Foundation for Strategic Research (SSF) via framework grant RMA08-0056. We gratefully acknowledge Gunnel Karlsson for her skilled work with the cryo-TEM. The authors also thank the Swedish synchrotron X-ray facility MAX-lab for allocating beamtime at the I911-4 beamline and Ana Labrador, Sylvio Haas, and Tomás Plivelic for technical support during experiments. Finally, Camurus AB is acknowledged for financial support.

■ ABBREVIATIONS

LCNP = liquid crystalline nanoparticle

SPC = soy phosphatidyl choline

GDO = glycerol dioleate

P80 = polysorbate 80

TGL = triacylglycerol lipase

■ REFERENCES

- (1) Luzzati, V.; Husson, F. The Structure of Liquid Crystalline Phases of Lipid–Water Systems. *J. Cell Biol.* **1962**, *12*, 207–219.
- (2) Seddon, J. M.; Templer, R. H. In *Handbook of Biological Physics*; Lipowsky, R.; Sackmann, E., Eds.; Elsevier Science B.V.: Amsterdam, 1995; Chapter 3, pp 97–160.
- (3) Guo, C.; Wang, J.; Cao, F.; Lee, R. J.; Zhai, G. Lyotropic Liquid Crystal Systems in Drug Delivery. *Drug Discovery Today* **2012**, *15*, 1032–1040.

(4) Cervin, C.; Tinzl, M.; Johnsson, M.; Abrahamsson, P.-A.; Tiberg, F.; Dizeyi, N. Properties and Effects of a Novel Liquid Crystal Nanoparticle Formulation of Docetaxel in a Prostate Cancer Mouse Model. *Eur. J. Pharm. Sci.* **2010**, *41*, 369–375.

(5) Cervin, C.; Vandoolaeghe, P.; Nistor, C.; Tiberg, F.; Johnsson, M. A Combined In Vitro and In Vivo Study on the Interactions between Somatostatin and Lipid-Based Liquid Crystalline Drug Carriers and Bilayers. *Eur. J. Pharm. Sci.* **2009**, *36*, 377–385.

(6) Tiberg, F.; Johnsson, M. Drug Delivery Applications of Non-lamellar Liquid Crystalline Phases and Nanoparticles. *J. Drug Delivery Sci. Technol.* **2011**, *21*, 101–109.

(7) Rizwan, S. B.; McBurney, W. T.; Young, K.; Hanley, T.; Boyd, B. J.; Rades, T.; Hook, S. Cubosomes Containing the Adjuvants Imiquimod and Monophosphoryl Lipid a Stimulate Robust Cellular and Humoral Immune Responses. *J. Controlled Release* **2013**, *165*, 16–21.

(8) Seddon, J. M. An Inverse Face-Centered Cubic Phase Formed by Diacylglycerol-Phosphatidylcholine Mixtures. *Biochemistry* **1990**, *29*, 7997–8002.

(9) Larsson, K. Cubic Lipid-Water Phases—Structures and Biomembrane Aspects. *J. Phys. Chem.* **1989**, *93*, 7304–7314.

(10) Gustafsson, J.; Ljusberg-Wahren, H.; Almgren, M.; Larsson, K. Submicron Particles of Reversed Lipid Phases in Water Stabilized by a Nonionic Amphiphilic Polymer. *Langmuir* **1997**, *13*, 6964–6971.

(11) Barauskas, J.; Misiunas, A.; Gunnarsson, T.; Tiberg, F.; Johnsson, M. “Sponge” Nanoparticle Dispersions in Aqueous Mixtures of Diglycerol Monooleate, Glycerol Dioleate, and Polysorbate 80. *Langmuir* **2006**, *22*, 6328–6334.

(12) Barauskas, J.; Cervin, C.; Jankunec, M.; Spandyreva, M.; Ribokaite, K.; Tiberg, F.; Johnsson, M. Interactions of Lipid-Based Liquid Crystalline Nanoparticles with Model and Cell Membranes. *Int. J. Pharm.* **2010**, *391*, 284–291.

(13) Das, S.; Rand, R. P. Diacylglycerol Causes Major Structural Transitions in Phospholipid Bilayer Membrane. *Biochem. Biophys. Res. Commun.* **1984**, *124*, 491–496.

(14) Das, S.; Rand, R. P. Modification by Diacylglycerol of the Structure and Interaction of Various Phospholipid Bilayer Membranes. *Biochemistry* **1986**, *25*, 2882–2889.

(15) Oradd, G.; Lindblom, G.; Fontell, K.; Ljusberg-Wahren, H. Phase-Diagram of Soybean Phosphatidylcholine-Diacylglycerol-Water Studied by X-ray Diffraction and P-31-NMR and Pulse Field Gradient H-1-NMR—Evidence for Reversed Micelles in the Cubic Phase. *Biophys. J.* **1995**, *68*, 1856–1863.

(16) Tiberg, F.; Johnsson, M.; Jankunec, J.; Barauskas, J. Phase Behavior, Functions, and Medical Applications of Soy Phosphatidylcholine and Diglyceride Lipid Compositions. *Chem. Lett.* **2012**, *41*, 1090–1092.

(17) Johnsson, M.; Barauskas, J.; Norlin, A.; Tiberg, F. Physicochemical and Drug Delivery Aspects of Lipid-Based Liquid Crystalline Nanoparticles—A Case Study of Intravenously Administered Propofol. *J. Nanosci. Nanotechnol.* **2006**, *6*, 3017–3024.

(18) Bode, J. C.; Kuntsche, J.; Funari, S. S.; Bunjes, H. Interaction of Dispersed Cubic Phases with Blood Components. *Int. J. Pharm.* **2013**, *448*, 87–95.

(19) Heller, F.; Reynaer, M.; Harv, C. Plasma Activities of Lipoprotein Lipase, Hepatic Lipase, and Lecithin: Cholesterol Acyltransferase in Patients Considered for Parenteral Nutrition with Fat Emulsion. *Am. J. Clin. Nutr.* **1985**, *41*, 748–752.

(20) Patton, S. J.; Carey, M. C. Watching Fat Digestion—The Formation of Visible Product Phases by Pancreatic Lipase Is Described. *Science* **1979**, *204*, 145–148.

(21) Barauskas, J.; Nylander, T. In *Delivery and Controlled Release of Bioactives in Foods and Neutraceuticals*; Garti, N., Ed.; Woodhead Publishing Ltd: Cambridge, 2008; Chapter 4, pp 107–131.

(22) Salentinig, S.; Sagalowicz, L.; Leser, M. E.; Tedeschi, C.; Glatter, O. Transitions in the Internal Structure of Lipid Droplets During Fat Digestion. *Soft Matter* **2011**, *7*, 650–661.

(23) Warren, D. B.; Anby, M. U.; Hawley, A.; Boyd, B. J. Real Time Evolution of Liquid Crystalline Nanostructure During the Digestion of

Formulation Lipids Using Synchrotron Small-Angle X-ray Scattering. *Langmuir* **2011**, *27*, 9528–9534.

(24) Luzzati, V.; Vargas, R.; Gulik, A.; Mariani, P.; Seddon, J. M.; Riva, E. Lipid Polymorphism: A Correction. The Structure of the Cubic Phase of Extinction Symbol $Fd\bar{}$ —Consists of Two Types of Disjoined Reverse Micelles Embedded in a Three-Dimensional Hydrocarbon Matrix. *Biochemistry* **1992**, *31*, 279–285.

(25) Delacroix, H.; Gulik-Krzywicki, T.; Seddon, J. M. Freeze Fracture Electron Microscopy of Lyotropic Lipid Systems: Quantitative Analysis of the Inverse Micellar Cubic Phase of Space Group $Fd\bar{3}m$ (Q227). *J. Mol. Biol.* **1996**, *258*, 88–103.

(26) Ruiz-Peña, M.; Oropesa-Núñez, R.; Pons, T.; Louro, S. R. W.; Pérez-Gramatges, A. Physico-Chemical Studies of Molecular Interactions between Non-ionic Surfactants and Bovine Serum Albumin. *Colloids Surf., B* **2010**, *75*, 282–289.

(27) Chang, D. P.; Jankunec, M.; Barauskas, J.; Tiberg, F.; Nylander, T. Adsorption of Lipid Liquid Crystalline Nanoparticles: Effects of Particle Composition, Internal Structure, and Phase Behavior. *Langmuir* **2012**, *29*, 10688–10696.

(28) Chang, D. P.; Jankunec, M.; Barauskas, J.; Tiberg, F.; Nylander, T. Adsorption of Lipid Liquid Crystalline Nanoparticles on Cationic, Hydrophilic, and Hydrophobic Surfaces. *ACS Appl. Mater. Interfaces* **2012**, *4*, 2643–2651.

(29) Barauskas, J.; Cervin, C.; Tiberg, F.; Johnsson, M. Structure of Lyotropic Self-Assembled Lipid Monolamellar Liquid Crystals and Their Nanoparticles in Mixtures of Phosphatidyl Choline and α -Tocopherol (Vitamin E). *Phys. Chem. Chem. Phys.* **2008**, *10*, 6483–6485.

(30) Barauskas, J.; Johnsson, M.; Joabsson, F.; Tiberg, F. Cubic Phase Nanoparticles (Cubosomes): Principles for Controlling Size, Structure and Stability. *Langmuir* **2005**, *21*, 2569–2577.

(31) Johnsson, M.; Lam, Y.; Barauskas, J.; Tiberg, F. Aqueous Phase Behavior and Dispersed Nanoparticles of Diglycerol Monooleate/Glycerol Doleate Mixtures. *Langmuir* **2005**, *21*, 5159–5165.

(32) Bagi, K.; Simon, L. M.; Szajáni, B. Immobilization and Characterization of Porcine Pancreas Lipase. *Enzyme Microb. Technol.* **1997**, *20*, 531–535.

(33) Schmid, R. D.; Verger, R. Lipases: Interfacial Enzymes with Attractive Applications. *Angew. Chem., Int. Ed.* **1998**, *37*, 1608–1633.

(34) Carrière, F.; Withers-Martinez, C.; van Tilbeurgh, H.; Roussel, A.; Cambillau, C.; Verger, R. Structural Basis for the Substrate Selectivity of Pancreatic Lipases and Some Related Proteins. *Biochim. Biophys. Acta* **1998**, *1376*, 417–432.

(35) Bergstrand, N.; Edwards, K. Aggregate Structure in Dilute Aqueous Dispersions of Phospholipids, Fatty Acids and Lysophospholipids. *Langmuir* **2001**, *17*, 3245–3253.

(36) Borné, J.; Nylander, T.; Khan, A. Microscopy, SAXD, and NMR Studies of Phase Behavior of the Monoolein–Dolein–Water System. *Langmuir* **2000**, *16*, 10044–10054.

(37) Borné, J.; Nylander, T.; Khan, A. Phase Behavior and Aggregate Formation for the Aqueous Monoolein System Mixed with Sodium Oleate and Oleic Acid. *Langmuir* **2001**, *17*, 7742–7751.

(38) Briggs, J.; Chung, H.; Caffrey, M. The Temperature-Composition Phase Diagram and Mesophase Structure Characterization of the Monoolein/Water System. *J. Phys. II* **1996**, *6*, 723–751.

(39) Edwards, K.; Silvander, M.; Karlsson, G. Aggregate Structure in Dilute Aqueous Dispersions of Oleic Acid/Sodium Oleate and Oleic Acid/Sodium Oleate/Egg Phosphatidylcholine. *Langmuir* **1995**, *11*, 2429–2434.